

Branching Structures in High-Pressure Low-Density Polyethylene as a Function of Molecular Weight Determined by ^{13}C Nuclear Magnetic Resonance and Pyrolysis-Hydrogenation Gas Chromatography

Takao Usami,* Yukitaka Gotoh, and Shigeru Takayama

Plastics Laboratory, Mitsubishi Petrochemical Co., Ltd., Tochocho-1, Yokkaichi, Mie Pref. 510, Japan

Hajime Ohtani and Shin Tsuge

Department of Synthetic Chemistry, Faculty of Engineering, Nagoya University, Furo-cho, Chikusa-ku, Nagoya 464 Japan. Received September 2, 1986

ABSTRACT: The type and content of branching in high-pressure low-density polyethylene (HPLDPE) as a function of molecular weight (MW) has been determined for a series of fractions of varying molecular weight prepared from one HPLDPE. Carbon-13 nuclear magnetic resonance (NMR) and pyrolysis-hydrogenation gas chromatography (PyHGC) have been employed for this purpose. From these results, it is clear that (i) the contents of total short-chain branches (SCBs), butyl branches, and ethyl branches increase steeply with decreasing MW in the low MW region, while the tendency becomes more gradual in the medium and high MW regions; (ii) the change of ethyl branch content as a function of MW is greater than that of butyl branches, so the amount of ethyl branches is larger in the low MW region and smaller in the high MW region than that of butyl branches; (iii) the concentrations of methyl branches incorporated by copolymerization with propylene and amyl branches are almost constant over all MW regions; and (iv) a considerable proportion of the chain ends are composed of the 3-ethyl structure in the low MW fractions.

Introduction

The mechanical properties of polymers are markedly affected not only by molecular weight (MW) and molecular weight distribution (MWD) but also by configurational and compositional variables. Practically, polymers should be considered as mixtures of molecules of varied molecular size and structure, so it would appear to be very important to investigate these distributions.¹

For a low-density polyethylene conventionally prepared under high pressure (HPLDPE), investigation of the type and content of short-chain branches (SCBs) and the content of long-chain branches (LCBs) as a function of MW has been considered to be of much interest in connection with HPLDPE physical properties and polymerization mechanisms. However, there have been only a few limited studies of the total SCB content by infrared analysis of branches as a function of MW.^{2,3}

Recent advances in analytical techniques have improved the situation. A series of ^{13}C nuclear magnetic resonance (NMR) studies for whole HPLDPEs have been reported.⁴⁻¹² ^{13}C NMR has the great advantage of being able to specifically identify a particular branch group and determine its content and location relative to the other branches. On the other hand, high-resolution pyrolysis-hydrogenation gas chromatography (PyHGC) has also played an important role for SCB analysis.¹³⁻¹⁹ PyHGC may have the advantages of minimal sample size and short analysis time in application to the fractionated sample.

In this paper, a commercial HPLDPE has been investigated by ^{13}C NMR and PyHGC for fractionated samples, and the type and content of branches as a function of MW have been determined.

Experimental Section

Sample. The characteristics of the parent HPLDPE investigated in this work are listed in Table I.

Fractionation. The fractionation was carried out by using a solvent gradient elution technique at a temperature (127 °C) above the melting point. The polymer was precipitated from xylene solution on Celite. A preheated good solvent (xylene)-poor solvent (ethylcellosolve) mixture was continuously dropped into the column at 127 °C, and the overflow effluent was collected.

The xylene content of the mixture employed was varied from about 35 to 61 vol %, and 16 fractions were obtained. Details of the fractions are listed in Table II.

Molecular Weight Determination. The number-average molecular weights (\bar{M}_n) for the parent polymer, fractions 4, 6, 8, 10, 12, and 15, were determined at 105 °C in 1,2,3,4-tetrahydronaphthalene by using a Hewlett-Packard high-speed membrane osmometer, Type 502, and the values are listed in Table II. The weight-average molecular weights (\bar{M}_w) for the whole polymer, fractions 12 and 15, were determined at 125 °C in α -chloronaphthalene by using a Shimadzu light-scattering instrument, Type PG-21.

Intrinsic Viscosity Measurement. The intrinsic viscosities ($[\eta]$) of fractions 12 and 15 were determined in 1,2,4-trichlorobenzene at 130 °C by using an inside dilution type Ubbelohde's viscometer.

^{13}C NMR and PyHGC Measurements. ^{13}C NMR measurements were carried out for the parent polymer, fractions 4, 6, 8, 10, 12, and 15. Pulse widths of 45° (9 μs) and pulse delay of 2 s were applied to about 10% (w/v) of the sample solution at 120 °C. A typical measurement was performed for 60–70 h for the fractions. PyHGC measurements were carried out for the fractions 1–13, 15, and 16. The PyHGC system utilized here is basically the same as that described previously.¹⁷ A sample size of about 500 μg was pyrolyzed at 710 °C under a flow of hydrogen carrier gas (50 mL/min). The degradation products were continuously hydrogenated in-line through a catalyst column and separated by a fused silica capillary column (0.2 mm i.d. \times 50 m) coated with immobilized poly(dimethylsiloxane) phase (OV-101). The column temperature was held initially at 40 °C for 2 min and programmed to increase at a rate of 2 °C/min up to 300 °C.

Determination of Branch Concentrations. The ^{13}C NMR measurement conditions used here do not completely satisfy the conditions for quantitative analysis pointed out by Axelson et al.,²⁰ but the T_1 values of the $\beta\text{-CH}_2$ carbons and the main- CH_2 carbons are not significantly different. For example, the $T_1(\beta\text{-CH}_2)$ are 1.4, 1.2, and 1.3 s and the $T_1(\text{main-CH}_2)$ are 1.6, 1.9, and 2.0 s for the ethylene/1-butene copolymer, the ethylene/1-hexene copolymer, and HPLDPEs, respectively.²⁰ The branch concentrations calculated from the integral intensities of $\beta\text{-CH}_2$ and main- CH_2 signals are almost the same for short- and long-pulse delay times.¹² Full NOEs are also expected for CH_2 carbons in the polymer main chain.²⁰ Therefore, it is reasonable to determine the branch concentrations from the integral intensities of $\beta\text{-CH}_2$ and main- CH_2 in the ^{13}C NMR spectra for the 2-s pulse delay. However, the concentration of each of the various branch types

Table I
Characteristics of the Parent HPLDPE

reactor	comonomer	$10^{-4}\bar{M}_n$	$10^{-4}\bar{M}_w$	branch contents per 1000 carbon atoms							
				total	$-\text{CH}_3$	$-\text{C}_2\text{H}_5$	$\begin{array}{c} \\ -\text{C}- \\ \\ \text{C}_2\text{H}_5 \end{array}$	$-\text{C}_3\text{H}_7$	$-\text{C}_4\text{H}_9$	$-\text{C}_5\text{H}_{11}$	longer ^a
tubular	propylene	4.0	27.8	24.6	2.9	5.5	2.0	0.4	7.3	3.0	3.5

^a Branches longer than pentyl and linear terminal methyls.

Table II
Fractionation Conditions and Characteristics of the Fractions

fraction	xylene, vol %	cumulative wt, %	\bar{M}_n	\bar{M}_w
1	35.0	0.7		
2	38.0	5.4		
3	41.0	12.2		
4	43.0	16.1	0.76	
5	46.0	19.5		
6	49.0	23.9	1.48	
7	52.0	30.3		
8	54.0	38.2	2.75	
9	55.0	47.3		
10	56.0	54.4	5.14	
11	57.0	61.1		
12	57.5	68.7	10.2	13.6
13	58.0	74.8		
14	59.0	79.7		
15	60.0	89.7	47.0	52.4
16	61.0	97.6		

cannot be determined for HPLDPE because the $\beta\text{-CH}_2$ signals of various branch types overlap. In order to determine the concentration of each branch type, a calibration technique was employed. The ^{13}C NMR spectrum of HPLDPE contains signals unique for each branch type. The concentrations and distribution of various branch types can be determined from the integral intensities of these signals. These integral intensities have been corrected using the intensity data for the carbons in ethylene/1-olefin copolymers for which the branch contents are known. The calibration factors for various carbons relative to the $\beta\text{-CH}_2$ content in the ethylene/1-olefin copolymers were determined using 2-s pulse delays.¹² With these values, the branch concentrations and distribution were calculated. The experimental errors in determining SCB and LCB contents by the calibration method are within 15% of the values.

Results and Discussion

A. SCBs (Short-Chain Branches). (1) ^{13}C NMR Results. Figure 1 shows partial spectra of the methyl signals from all types of branches for fractions 4, 6, 8, 10, 12, and 15. The pattern of these spectra does not change markedly from fraction to fraction. The methyl signal from ethyl branches at 11.01 ppm was assigned to 1,3-paired ethyl branches¹² and/or 2-ethylhexyl branches,²¹ and the signals from ethyl branches attached to quaternary carbon atoms were also recognized around 8 ppm in all fractions. Since propylene was copolymerized as a MW

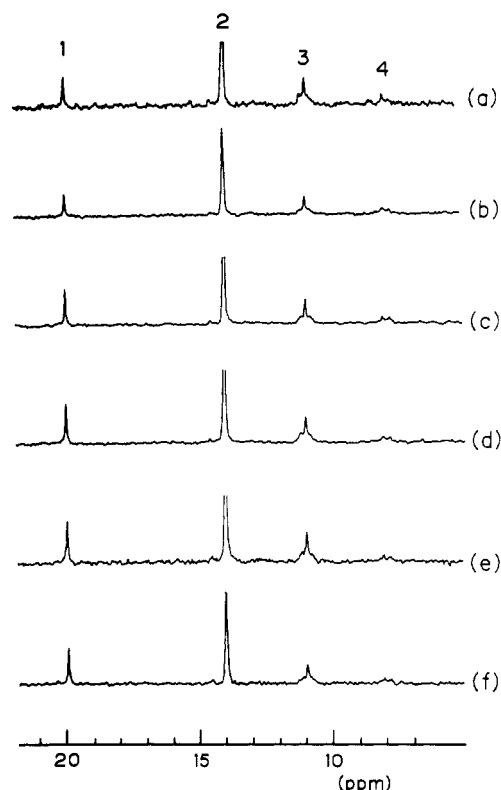


Figure 1. Methyl signal region in ^{13}C NMR spectra of the fractions: (1) methyl branches, (2) butyl branches and branches longer than butyl, (3) ethyl branches, (4) ethyl branches attached to a quaternary carbon; (a) fraction 4, (b) fraction 6, (c) fraction 8, (d) fraction 10, (e) fraction 12, (f) fraction 15.

modifier, the signal from methyl branches at 19.98 ppm was clearly observed. Quantitative results for all types of branches are listed in Table III. The branch contents as a function of MW, shown in Figure 2, demonstrate that (a) the contents of total SCBs, butyl branches, and ethyl branches increase steeply with decreasing MW in low MW region, while the tendency becomes more gradual in medium and high MW regions; (b) the change of ethyl branch content as a function of MW is greater than that of butyl branches and the amount of ethyl branches is larger in the low MW region and smaller in the high MW region than that of butyl branches; and (c) the contents of methyl

Table III
Branch Distributions Determined by ^{13}C NMR for the HPLDPE Fractions

fraction	branch contents per 1000 carbon atoms							
	total	$-\text{CH}_3$	$-\text{C}_2\text{H}_5$	$\begin{array}{c} \\ -\text{C}- \\ \\ \text{C}_2\text{H}_5 \end{array}$	$-\text{C}_3\text{H}_7$	$-\text{C}_4\text{H}_9$	$-\text{C}_5\text{H}_{11}$	longer ^a
4	31.3	2.9	7.7	3.3	0.9	9.0	3.1	4.4
6	28.1	3.1	6.0	3.0	0.9	8.5	3.0	3.6
8	25.4	2.8	5.9	2.1	0.6	7.8	2.9	3.3
10	22.7	2.5	5.2	1.8	0.4	7.1	2.6	3.1
12	22.2	2.8	4.8	1.7	0.6	7.0	2.4	2.9
15	22.2	3.0	4.4	1.3	0.7	7.1	2.6	3.1

^a Branches longer than pentyl and linear terminal methyls.

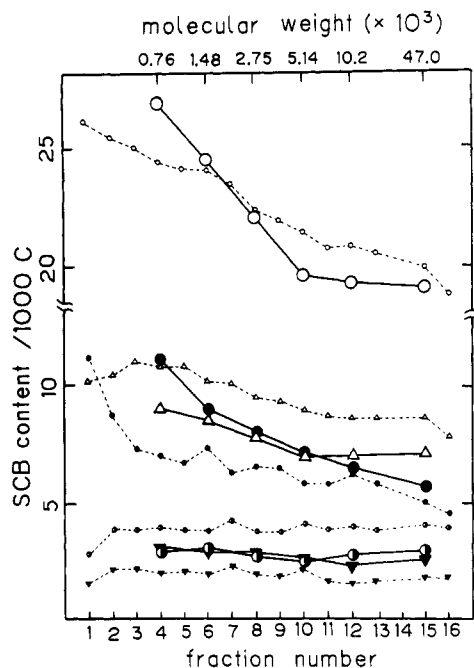


Figure 2. SCB contents in HPLDPE fractions determined by ^{13}C NMR (—) and by PyHGC (—); (○) total SCB, (Δ) butyl branch, (●) ethyl branch, (○) methyl branch, (▼) amyl branch.

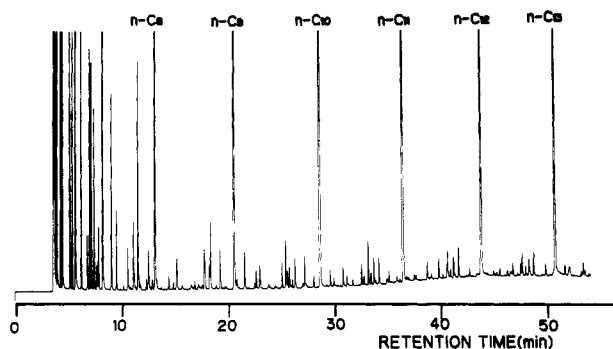


Figure 3. High-resolution pyrogram of a fraction of HPLDPE (fraction 12) at 710 °C.

branches incorporated by copolymerization with propylene and amyl branches are almost constant all over MW regions.

(2) **PyHGC Results.** Figure 3 shows a typical high-resolution pyrogram for a fraction. The SCB contents in the fractions were determined from the relative peak intensities of the characteristic isoalkanes in the C_{11} fragment region by comparing the data obtained with reference model ethylene/1-olefin copolymers, as reported previously.¹⁹ Figure 4 represents the expanded partial pyrograms of a low MW fraction (Fraction 2) and a high MW fraction (fraction 12) in the C_{11} region. The relative peak intensities of 5-ethylnonane (5E) and 3-methyldecane (3M), which are characteristic of ethyl branches, are apparently higher in the low MW fractions.

The SCB contents determined by PyHGC are summarized in Table IV. Figure 2 illustrates the SCB contents in the HPLDPE fractions determined by ^{13}C NMR and PyHGC as a function of MW for the fractions. The general trends of the total and individual branch contents as a function of MW are in fairly good agreement for the two methods. However, each content determined by PyHGC deviates to some extent from that determined by ^{13}C NMR. This discrepancy is considered mainly to be caused by the assumption made in PyHGC that the ethyl branches in HPLDPE are randomly placed along the chain

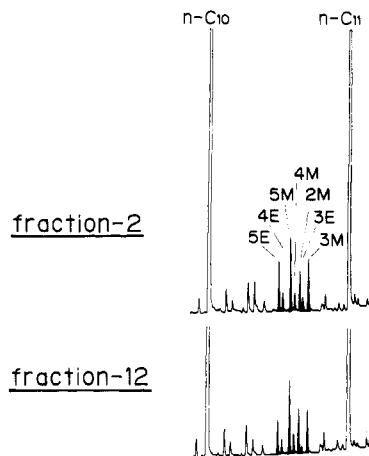


Figure 4. Expanded partial pyrograms of fraction 2 and fraction 12 in the C_{11} region: (2M) 2-methyldecane, (3M) 3-methyldecane, (4M) 4-methyldecane, (5M) 5-methyldecane, (3E) 3-ethyldecane, (4E) 4-ethyldecane, (5E) 5-ethyldecane.

Table IV
Branch Distributions Determined by PyHGC for the HPLDPE Fractions

fraction	branch contents per 1000 carbon atoms					
	total	— CH_3	— C_2H_5	— C_4H_9	— C_5H_{11}	— C_6H_{13}
1	26.2	2.9	11.2	10.2	1.7	0.2
2	25.6	3.9	8.7	10.4	2.3	0.3
3	25.0	4.0	7.3	11.0	2.3	0.4
4	24.4	4.1	7.0	10.8	2.1	0.4
5	24.1	3.9	6.7	10.8	2.2	0.5
6	24.1	3.9	7.3	10.2	2.1	0.6
7	23.5	4.3	6.3	10.1	2.4	0.4
8	22.3	3.8	6.5	9.5	2.1	0.4
9	21.9	3.8	6.5	9.3	2.0	0.3
10	21.4	4.1	5.8	8.9	2.3	0.3
11	20.7	3.9	5.9	8.7	1.8	0.4
12	20.8	4.0	6.2	8.6	1.7	0.3
13	20.5	3.9	5.8	8.6	1.8	0.4
15	19.9	4.1	5.0	8.6	1.9	0.3
16	18.8	4.0	4.6	7.8	2.0	0.4

Table V
Observed and Calculated Peak Intensities of 5-Ethylnonane (5E) and 3-Ethylnonane (3E)

fraction	$I_{\text{obsd}}(5\text{E})^a$	$I_{\text{calcd}}(5\text{E})^b$	$I_{\text{obsd}}(3\text{E})^a$	$I_{\text{calcd}}(3\text{E})^b$
1	29.5	12.3	10.9	9.1
2	28.2	11.5	8.8	7.1
3	25.5	11.5	6.6	6.0
4	23.2	11.2	5.8	5.8
5	23.4	11.1	5.4	5.6
6	22.2	10.8	5.1	6.1
8	20.0	10.0	4.4	5.4
10	17.9	9.2	3.6	4.8
12	16.5	9.2	3.5	5.1
15	17.0	8.8	3.9	4.2

^a Observed intensities relative to $I_{\text{obsd}}(n\text{-C}_{11}) = 1000$. ^b $I_{\text{calcd}}(5\text{E}) = \sum_i C_i/f_i(5\text{E})$ and $I_{\text{calcd}}(3\text{E}) = \sum_i C_i/f_i(3\text{E})$, where i = each branching (methyl, ethyl, butyl, pentyl and hexyl), C_i = i branch content/1000 C of the fraction determined by PyHGC (values in Table IV), and f_i = correlation factor calculated from the relative peak intensity of 5E (or 3E) on the pyrogram of the model copolymer with known i branch content by using the equation¹⁶, $I_{\text{obsd}}(5\text{E})/f_i(5\text{E}) = I_{\text{obsd}}(3\text{E})/f_i(3\text{E}) = i$ branch number/1000 C.

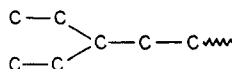
rather than paired and/or branched as shown by ^{13}C NMR.¹² As shown in Table V, this is confirmed by the fact that the observed peak intensities of 5E, which is preferentially formed from the paired and/or branched ethyl branch structures compared to isolated ones, are much larger than those calculated from the estimated branch contents by PyHGC, assuming random distribution of the SCB along the polymer chain.¹⁹ Therefore, the conclusions

Table VI
LCB Contents Determined by the ^{13}C NMR and the
Viscosity Methods for the HPLDPE Fractions

fraction	LCB contents/ 1000 C (by ^{13}C NMR)	LCB contents/1000 C by the viscosity method			
		$\epsilon = 0.5$	$\epsilon = 0.75$	$\epsilon = 1.0$	$\epsilon = 1.5$
8	2.8				
10	2.9				
12	3.1	3.1	1.4	0.85	0.45
15	3.4	9.5	2.4	1.1	0.45

derived from ^{13}C NMR results are confirmed by the PyHGC results.

On the other hand, 3-ethylnonane (3E) is considered difficult to form from paired and/or branched branches, but the observed intensities of 3E are higher than those calculated by assuming isolated ethyl branches in the low MW region, as shown in Table V. This fact suggests that there might exist a considerable proportion of 3-ethyl chain ends



in the HPLDPE sample, because 3E might predominantly arise from such chain ends in the low MW region, where relative concentrations of chain ends are much higher than in medium and high MW regions.

The constancy of methyl branch content regardless of MW implies that MW reduction by the modifier took place with almost the same probability for all molecules. The steep increase of complex ethyl branch content, such as 1,3-paired ethyl and 2-ethylhexyl, in the low MW region implies that the low MW component of HPLDPE is polymerized at a higher temperature than the high MW component. There are two different reports on the SCB content as a function of MW so far. Shirayama et al.² obtained the results that the degree of SCB increases with decreasing MW, while Otocka et al.³ obtained the reverse results. Our results clearly support the former, and the lower MW molecules are considered to be produced in the higher temperature region.

B. LCBs (Long-Chain Branches). (1) ^{13}C NMR Results. It is well-known that LCBs are detected directly by ^{13}C NMR.^{8,10,12} The amounts of LCBs have been determined for the fractions 8, 10, 12, and 15 by

$$A_{\text{LCB}} = (X + Z) - Y$$

where A_{LCB} is the content of LCBs, X is the content of all the methyl-type chain ends greater than six carbons in length determined by ^{13}C NMR from the signal at 32.2 ppm, and Z is the content of the vinyl-type chain ends determined by infrared. $(X + Z)$ is the content of all chain ends including the chain ends of the main chain and the LCBs. The content of the chain ends of the main chain, Y , is determined from the value of M_n by assuming that the polymer has two end groups. The LCB results by ^{13}C NMR in Table VI show that the extent of long-chain branching gradually increases with increasing MW.

(2) **Intrinsic Viscosity Method.** The amount of LCB has also been determined by intrinsic viscosity measurements.²² Solution viscosity is related to molecular structure by $g' = [\eta]_b/[\eta]_l$,²³ where $[\eta]_b$ and $[\eta]_l$ are the intrinsic viscosities of branched and linear molecules at the same MW, respectively, g is the ratio of the mean-square radius of gyration of the branched molecules to that of the linear molecules, and ϵ is a variable parameter ranging from 0.5 to 1.5. For example, ϵ is 0.5 for star-shaped molecules²⁴ and 1.5 for linear molecules.²⁵ The amounts of LCBs per

MW unit, λ , were related to the ratio of the mean-square radii of gyration, g , for monodisperse molecules by²⁶

$$g = \left[\left(1 + \frac{\lambda M}{7} \right)^{1/2} + \frac{4}{9\pi} \lambda M \right]^{-1/2}$$

The contents of LCBs were determined only for fractions 12 and 15 because satisfactory accuracy of the results could not be obtained for the lower MW fractions. Since the contents of LCBs depend upon the value of ϵ , the contents were determined for four ϵ values (0.5, 0.75, 1.0, and 1.5). The results are shown in Table VI.

The ^{13}C NMR LCB determination may or may not agree with the viscosity method because the ^{13}C NMR method covers branches of seven carbons and longer. However, since no appreciable amount of hexyl branches is present in HPLDPEs,¹² it can be assumed that the contribution of intermediate-length branches (hexyl, heptyl, octyl, etc.) does not cause significant error in the estimation of LCBs in HPLDPE by ^{13}C NMR. Therefore, the comparison of the LCB values by the two different methods seems to be meaningful.

The trend of the LCB content as a function of MW is in good agreement by ^{13}C NMR and the viscosity methods for $\epsilon = 1.0$. However, the amounts by the viscosity method are about one-third of those obtained by ^{13}C NMR. For $\epsilon = 0.5$, the trend as a function of MW is completely different between ^{13}C NMR and the viscosity methods, being much smaller by ^{13}C NMR for fraction 15. Therefore, the value of ϵ does not seem to be near 0.5. Except for the case of $\epsilon = 0.5$, the amount of LCB by ^{13}C NMR tends to be larger than that by the viscosity method. This tendency might be due to the existence of rather short LCBs which do not contribute to the results by the viscosity method. However, further investigations are necessary to permit a precise comparison between the LCB results by ^{13}C NMR and the solution method.

Conclusions

SCB and LCB as a function of MW have been investigated for the MW-fractionated samples of one sample of HPLDPE by ^{13}C NMR, PyHGC, and the intrinsic viscosity method, and the following conclusions have been obtained.

(1) The contents of total SCBs, butyl branches, and ethyl branches increase steeply with decreasing MW in the low MW region, while the tendency becomes more gradual in the medium and high MW regions.

(2) The change of ethyl branch content as a function of MW is greater than that for butyl branches, so the amount of ethyl branches is larger in the low MW region and smaller in the high MW region than that of butyl branches.

(3) The types of ethyl branches are mainly 1,3-paired ethyl and/or 2-ethylhexyl and ethyl branches attached to quaternary carbon atom in all MW regions.

(4) Methyl branches incorporated by copolymerization with propylene and amyl branch contents are almost constant over all MW regions.

(5) The general tendencies for the total and individual SCB contents as a function of MW are in good agreement between the ^{13}C NMR and PyHGC methods.

(6) A considerable proportion of the chain ends may be composed of the 3-ethyl structure in the low MW fractions.

(7) LCB contents determined by ^{13}C NMR gradually increase with increasing MW and seem to be different from those by the intrinsic viscosity method in the tendency as a function of MW.

Acknowledgment. We thank John Summers and Hisao Umemoto for their assistance in preparing the manuscript and Mitsubishi Petrochemical Co. for per-

mission to publish this work.

Registry No. (E)(P) (copolymer), 9010-79-1.

References and Notes

- (1) Mirabella, F. M., Jr.; Johnson, J. F. *J. Macromol. Sci., Rev. Macromol. Chem.* **1975**, C12, 81.
- (2) Shirayama, K.; Okada, T.; Kita, S. *J. Polym. Sci., Part A* **1965**, A3, 907.
- (3) Otocka, E. P.; Roe, R. J.; Hellman, M. Y.; Muglia, P. M. *Macromolecules* **1971**, 4, 507.
- (4) Dorman, D. E.; Otocka, E. P.; Bovey, F. A. *Macromolecules* **1972**, 5, 574.
- (5) Randall, J. C. *J. Polym. Sci., Polym. Phys. Ed.* **1973**, 11, 275.
- (6) Hama, T.; Suzuki, T.; Kosaka, K. *Kobunshi Ronbunshu* **1975**, 32, 91.
- (7) Cudby, M. E. A.; Bunn, A. *Polymer* **1976**, 17, 345.
- (8) Bovey, F. A.; Schilling, F. C.; McCrackin, F. L.; Wagner, H. L. *Macromolecules* **1976**, 9, 76.
- (9) Cheng, H. N.; Schilling, F. C.; Bovey, F. A. *Macromolecules* **1976**, 9, 363.
- (10) Axelson, D. E.; Levy, G. C.; Mandelkern, L. *Macromolecules* **1979**, 12, 41.
- (11) Nishioka, A.; Mukai, Y.; Ohuchi, M.; Imanari, T. *Bunseki Kagaku* **1980**, 29, 774.
- (12) Usami, T.; Takayama, S. *Macromolecules* **1984**, 17, 1756.
- (13) Seeger, M.; Barrall, E. M. *J. Polym. Sci., Polym. Chem. Ed.* **1975**, 13, 1515.
- (14) Ahlstrom, D. H.; Liebman, S. A.; Abbas, K. B. *J. Polym. Sci., Polym. Chem. Ed.* **1976**, 14, 2479.
- (15) Sugimura, Y.; Tsuge, S. *Macromolecules* **1979**, 12, 512.
- (16) Tsuge, S.; Sugimura, Y.; Nagaya, T. *J. Anal. Appl. Pyrolysis* **1980**, 1, 221.
- (17) Sugimura, Y.; Usami, T.; Nagaya, T.; Tsuge, S. *Macromolecules* **1981**, 14, 1787.
- (18) Liebman, S. A.; Ahlstrom, D. H.; Starnes, W. H.; Schilling, F. C. *J. Macromol. Sci., Chem.* **1982**, A17, 935.
- (19) Ohtani, H.; Tsuge, S.; Usami, T. *Macromolecules* **1984**, 17, 2557.
- (20) Axelson, D. E.; Mandelkern, L.; Levy, G. C. *Macromolecules* **1977**, 10, 557.
- (21) Grenier-Loustalot, M.-F. *J. Polym. Sci., Polym. Chem. Ed.* **1983**, 21, 2683.
- (22) (a) Billmeyer, F. W., Jr. *J. Am. Chem. Soc.* **1953**, 75, 6118. (b) Drott, E. E.; Mendelson, R. A. *J. Polym. Sci., Part A-2* **1970**, 8, 1361, 1373.
- (23) Zimm, B. H.; Kilb, R. W. *J. Polym. Sci.* **1959**, 37, 19.
- (24) Morton, M.; Helminiak, T. E.; Gadkary, S. D.; Bueche, F. J. *Polym. Sci.* **1962**, 57, 471.
- (25) Flory, P. J.; Fox, T. G. *J. Am. Chem. Soc.* **1951**, 73, 1904.
- (26) Zimm, B. H.; Stockmayer, W. H. *J. Chem. Phys.* **1949**, 17, 1301.

Characterization of Thermal Diffusion in Polymer Solutions by Thermal Field-Flow Fractionation: Effects of Molecular Weight and Branching

Martin E. Schimpf and J. Calvin Giddings*

Department of Chemistry, University of Utah, Salt Lake City, Utah 84112.

Received December 8, 1986

ABSTRACT: Thermal field-flow fractionation has been applied to 29 linear and branched polystyrene samples dissolved in ethylbenzene. The samples varied widely in chain length and branching configuration. The dependence of retention on the molecular weight and the ordinary diffusion coefficient was established. It is shown from these results that the thermal diffusion coefficient is essentially constant, independent of both molecular weight and the form of branching. This result is consistent with the theoretical conclusions of Brochard and de Gennes.

Introduction

The thermal diffusion of polymers in solution is an intrinsically interesting transport phenomenon, but it is poorly understood and infrequently studied. However, thermal diffusion has gained in practical importance recently because it underlies the technique of thermal field-flow fractionation (thermal FFF or ThFFF). Fortunately, every ThFFF experiment is capable of producing thermal diffusion data. In this way ThFFF has become the best technique for the systematic study of thermal diffusion and thus of its own foundations.

ThFFF is a technique applicable to the separation and characterization of polymeric materials.¹⁻³ In this technique a thin pulse of dilute polymer sample is carried by flow along a narrow ribbonlike channel across which an external "field" in the form of a thermal gradient is applied. The velocity profile of the carrier liquid in the channel is near parabolic, with a higher flow velocity in the channel center than near the walls. The polymer, under the influence of the temperature gradient, is forced toward the cold wall. The resulting buildup of concentration at the cold wall is opposed by ordinary diffusion, and a dynamic steady-state condition is reached in which the field-induced motion is balanced against back-diffusion.

The spatial distribution of polymer formed at the cold wall under this steady-state condition is exponential in form and can be characterized by the effective thickness l , the distance from the cold wall to the center of gravity of the polymer zone. The parameter l is typically expressed in the dimensionless form $\lambda = l/w$, where w is the channel thickness or distance between hot and cold walls. The constant λ is termed the retention parameter and can be related, by considering the flow profile, to the experimental retention volume V_r , the volume of carrier solvent required to transport the polymer through the length of the channel. For parabolic flow³

$$R = V^0/V_r = 6\lambda(\coth(1/2\lambda) - 2\lambda) \quad (1)$$

where R is the retention ratio and V^0 is the channel void volume. Clearly, each experimental measurement of V_r yields a unique value of λ . Equation 1 must be corrected somewhat to account for the departure from parabolic flow induced by the temperature gradient and attendant viscosity changes in the channel.⁴

The variation of retention parameter λ among different polymers can be attributed to changes both in thermal diffusion and in ordinary diffusion. The relationship of λ to the corresponding transport coefficients is given by³